AD-A177 928 TURBULENT FLOW OVER AN EMBEDDED RECTANGULAR CAVITY(U) 1/1
AIR FORCE ARMAMENT LAB EGLIN AFB FL G D CATALANO
FEB 87 AFATL-TR-86-73 SBI-AD-E001 466

UNCLASSIFIED F/G 20/4 NL

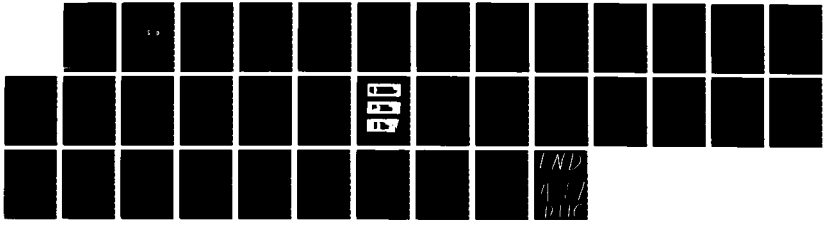

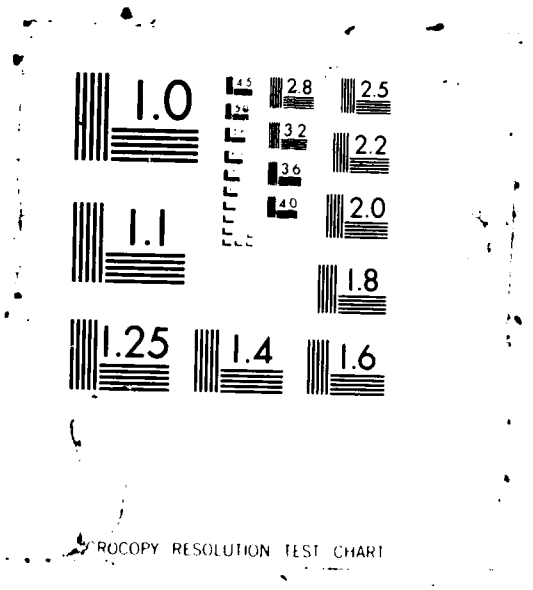
1.0
1.1
1.25
1.4
1.6
2.8
2.5
3.2
2.2
3.6
2.0
4.0
1.8
ROCOPY RESOLUTION TEST CHART

EF01466

(2)

AFATL-TR-86-73

Turbulent Flow Over an Embedded Rectangular Cavity

George D Catalano

AERODYNAMICS BRANCH
AEROMECHANICS DIVISION

DTIC
ELECTE
MAR 1 8 1987
S D
D

AD-A177 928

FEBRUARY 1987

FINAL REPORT FOR PERIOD JUNE 1986-SEPTEMBER 1986

APPROVED FOR PUBLIC RELEASE; DISTRIBUTION UNLIMITED

DESTRUCTION NOTICE: DESTROY BY ANY METHOD THAT WILL PREVENT DISCLOSURE OF CONTENTS OR RECONSTRUCTION OF THE DOCUMENT.

AIR FORCE ARMAMENT LABORATORY
Air Force Systems Command ▮ United States Air Force ▮ Eglin Air Force Base, Florida

DTIC FILE COPY

87 3 1

UNCLASSIFIED
SECURITY CLASSIFICATION OF THIS PAGE

AD-A177928

REPORT DOCUMENTATION PAGE

1a. REPORT SECURITY CLASSIFICATION UNCLASSIFIED	1b. RESTRICTIVE MARKINGS N/A
2a. SECURITY CLASSIFICATION AUTHORITY N/A	3. DISTRIBUTION/AVAILABILITY OF REPORT Approved for public release; distribution is unlimited.
2b. DECLASSIFICATION/DOWNGRADING SCHEDULE	
4. PERFORMING ORGANIZATION REPORT NUMBER(S) AFATL-TR-86-73	5. MONITORING ORGANIZATION REPORT NUMBER(S) AFATL-TR-86-73
6a. NAME OF PERFORMING ORGANIZATION Aeromechanics Division 6b. OFFICE SYMBOL (If applicable) FXA	7a. NAME OF MONITORING ORGANIZATION Aerodynamics Branch Aeromechanics Division
6c. ADDRESS (City, State and ZIP Code) Air Force Armament Laboratory Eglin Air Force Base, Florida 32542-5434	7b. ADDRESS (City, State and ZIP Code) Air Force Armament Laboratory Eglin Air Force Base, Florida 32542-5434
8a. NAME OF FUNDING/SPONSORING ORGANIZATION Air Force Office of Scientific Research 8b. OFFICE SYMBOL (If applicable) AFOSR	9. PROCUREMENT INSTRUMENT IDENTIFICATION NUMBER
8c. ADDRESS (City, State and ZIP Code) Bolling AFB DC 20332	10. SOURCE OF FUNDING NOS. PROGRAM ELEMENT NO. 61102F; PROJECT NO.; TASK NO.; WORK UNIT NO.
11 TITLE (Include Security Classification) Turbulent FLow Over an Embedded Rectangular Cavity	
12. PERSONAL AUTHOR(S) George D. Catalano	
13a. TYPE OF REPORT Final 13b. TIME COVERED FROM 30 Jun 85 TO 5 Sep 86	14 DATE OF REPORT (Yr., Mo., Day) 1987 February 15. PAGE COUNT 32
16. SUPPLEMENTARY NOTATION Availability of this report is specified on verso of front cover.	
17 COSATI CODES FIELD 20; GROUP 04; SUB GR	18. SUBJECT TERMS (Continue on reverse if necessary and identify by block number) 3 Dimensional Turbulent Cavity Flow Cavity, Cavity Flow Field, Vortex Model

19 ABSTRACT (Continue on reverse if necessary and identify by block number)

A numerical, discrete vortex model is developed for flow over an embedded rectangular cavity, with the separation of the shear layer at the leading edge replaced by periodic insertion of point vortices. The results of the vortex model are compared to the data obtained from an experimental investigation carried out at a free stream speed of 6 m/sec past a rectangular cavity of depth, D equal to 5 cm; a depth-to-width ratio, D/W equal to 1.0 and length-to-depth ratio, L/D, equal to 4.0. The Reynolds numbers based on the cavity depth is approximately 2×10^4. Mean velocity, and turbulent intensity, profiles are presented. Evidence of the three dimensional nature of the flow has been obtained via oil film and tuft flow visualization techniques. Discrepancies between the model predictions and the experimental results are discussed as are differences between the 3-D flow field examined here and previous infin.te span, 2-D, cavity configurations. Additionally, a mechanism is developed for the inclusion in the vortex model of various initial separation conditions.

20 DISTRIBUTION/AVAILABILITY OF ABSTRACT UNCLASSIFIED/UNLIMITED ☒ SAME AS RPT ☐ DTIC USERS ☐	21 ABSTRACT SECURITY CLASSIFICATION UNCLASSIFIED
22a. NAME OF RESPONSIBLE INDIVIDUAL Carroll B. Butler	22b TELEPHONE NUMBER (Include Area Code) (904) 882-5652 22c OFFICE SYMBOL AFATL/FXA

DD FORM 1473, 83 APR EDITION OF 1 JAN 73 IS OBSOLETE

UNCLASSIFIED
SECURITY CLASSIFICATION OF THIS PAGE

PREFACE

This report describes an in-house effort monitored by Mr Carroll Butler of the Aerodynamics Branch (FXA), Aeromechanics Division (FX), Air Force Armament Laboratory, Eglin AFB, Florida, under project 25670320, "Weapons Internal Carriage/Separations (WICS)." The work reported herein was performed during the period 30 June to 5 September 1986 by Dr George Catalano from Louisiana State University. The effort was sponsored by AFOSR under the Summer Research Faculty Program.

This report is one portion of a planned number of efforts addressing the internal carriage and separation of stores from high performance aircraft.

Dr Catalano would like to thank the Air Force Systems Command and the Air Force Office of Scientific Research for sponsorship of the research. He would also like to express appreciation to his sponsor, Mr Carroll Butler, Technical Advisor, and Mr Steve Korn, Branch Chief, of the Aerodynamics Branch, Armament Laboratory for providing the environment that is a prerequisite for the search of new ideas.

This report was edited and published under the auspices of the Air Force Armament Laboratory (DOIR), Air Force Systems Command, United States Air Force, Eglin Air Force Base, Florida.

Accesion For
NTIS CRA&I ☒
DTIC TAB ☐
Unannounced ☐
Justification .....
By .....
Distribution /
Availability Codes
Dist | Avail and / or Special
A-1

DTIC COPY INSPECTED 5

(The reverse of this page is blank)

TABLE OF CONTENTS

LIST OF FIGURES

NOMENCLATURE

A	constant
A/R	aspect ratio (D/L)
D	cavity depth
E(.)	complete elliptical integral of the second kind
E(·/·)	incomplete elliptical integral of the second kind
L	cavity length
N	number of vortices
U,V	mean velocity components in the stream and cross-stream direction
U_{max}	free stream velocity
V	angular component of velocity
V_r	radial component of velocity
W	cavity width
a	position of transformed cavity corner
f'(.)	first derivative of transformal function
f"(.)	second derivative of transformal function
k	wave number
m,n	integer
r	distance from the center of vortex
t	dimensionless time
u,v	turbulent fluctuation components
x,y	dimensionless Cartesian coordinates
z	complex variable in the physical coordinate system
Γ	circulation of vortices
Δt	dimensionless time step
λ	transformed complex variable, wavelength
ν	kinematic viscosity

ρ	density
ω	vorticity
$*$	complex conjugate

SECTION I
INTRODUCTION

1. OVERALL OBJECTIVE OF RESEARCH EFFORT

The overall objective of the research effort is a more precise understanding of turbulent flow past an embedded, rectangular cavity.

Flow past embedded cavities are examples of separated flows which are of significant engineering interest. There is considerable progress to be made in the understanding of the dynamics behavior of such flow fields. A weapons bay exposed to the outer flow is an example of the existence and importance of such flow fields. The flow field within the bay affects the initial behavior of the mounted weapons at the crucial release time. Also, coupling of the self-sustaining oscillations present in some cavity flows with the resonant frequencies of nearby aircraft structures could result in serious structural damage. An additional example of the relevance of the flow configuration in addition to a weapons bay can be seen in airborne open viewing ports which can be required for various optical devices such as infrared telescope sensors, or lasers. When exposed to the freestream flow, the open viewing ports act as cavities which can result in unwanted internal vibrations generated by the unsteady, turbulent pressure and velocity fields. Flow field spoilers have been successfully used ahead of open viewing ports in order to acoustically quiet an open-port cavity yet their application seems adhoc at best. Thus, one desired outcome of the investigation is to formulate the open cavity flow in such a manner as to enable the engineer the opportunity to estimate the sensitivity of resultant turbulent field to an important initial condition, i.e., the mean velocity profile at the point of separation.

A second desired outcome of the investigation is to determine the effects of a finite width on the flow past an embedded cavity. There is a serious shortage of such experimental data at the present time.

A number of numerial and experimental investigation of 2-D flow past cavities and backward facing steps have been reported. For low Reynolds number flows, numerial studies by Kawagutti, Reference 1, Mills, Reference 2, Burgraf, Reference 3, Pan and Acrivos, Reference 4, Nallaswamy and Prasad, Reference 5, and Bozeman and Dalton, Reference 6, have been reported, though frequently the free surface boundary condition had to be changed such that the flow is induced by a top moving wall. Sarohia, Reference 7, experimentally investigated laminar separation flow over axisymmetric rectangular cavities and found that the depth-to-length ratio can be used to characterize cavity flow as open or closed in an analogous manner as in the turbulent case.

For the case of larger Reynolds numbers, Roshko, Reference 8, Tani, et.al., Reference 9, Sinha, et.al, Reference 10, and Rockwall and Kinsley, Reference 11 experimetally studied boundary layer flows over embedded cavities with concentration on the overall features of the flow such as velocity and surface pressure distributions, skin friction variations, and interfacial stability. Hankey and Shang (Reference 12) and Gatski et.al., Reference 13) numerically studied the high speed shear flow driven cavity problem.

SECTION II
MATHEMATICAL AND NUMERICAL FORMULATION

A general framework for describing cavity flows and the resultant flow oscillations is given by Rockwell and Naudascher (Reference 14). The fluid dynamic oscillations which are primarily attributable to the instability of the cavity shear layer are the focus of this investigation. These oscillations can be traced from the initial disturbances and vortical fluctuations in the cavity shear layer. The disturbances are then enhanced by the feedback mechanism at the downstream edge of the cavity.

The mathematical approach taken here is the development of a potential model of the complete cavity flow. The flow separates at the leading edge of the cavity, creating a highly vortical shear layer between the fluid within the cavity and the outer free stream. The shear layer diffuses into the cavity, eventually impinging upon the rear wall, and turning downwards creating a large trapped vortex. This vortex which is fed energy by the shear layer interacts with the interfacial region inducing a semiperiodic displacement of the shear layer which in turn governs the rate at which vorticity is shed downstream.

The main tenet of the potential model is that the free shear layer, which separates at the cavity leading edge, can be replaced by periodic insertion of point vortices at or near the separation point. The discrete vortex approximation utilizes a Schwarz-Christoffel transformation to map the cavity geometry onto the upper half plane. The strength of the discrete vortices is determined from the application of the Kutta condition at the leading edge with the zero normal velocity at the walls satisfied by the insertion of image vortices.

The first representation of a continuous vortex sheet by discrete vortices was presented by Rosenhead (Reference 15), with later improvements made by Birkhoff and Fisher (Reference 16). The development and interaction of two vortex layers was described by Abernathy and Kronauer (Reference 17) and Moor (Reference 18). The first application of a discrete vortex representation of a shear layer for flow around a bluff body was performed by Gerrard (Reference 19), and later by Sarpkaya (Reference 20) and Laird (Reference 21) for the case of flow around a circular cylinder.

An inviscid model of two dimensional vortex shedding behind a square-based section was developed by Clements and Maull (Reference 22-24) and extended by Hardin and Mason (Reference 25) to squa cavities and by Davies, et al.

(Reference 26) and Bradshaw, et al. (Reference 27) to jet flows. The discrete vortex model developed by Clements (Reference 22) and Hardin (Reference 25) forms the basis of the model developed in this investigation.

DISCRETE VORTEX MODEL

The flow over the embedded cavity is modelled by a series of discrete vortices superimposed onto irrotational inviscid flow. Consider a two dimensional cavity of length L, and depth D with the assumption that for upstream and for downstream from the cavity, the flow is uniform and parallel (Figure 1). A Schwarz-Cristoffel transformation is used to map the cavity onto the transformed λ -plane. That is,

$$Z = E\,[\sin^{-1}(\lambda)/\sin^{-1}(1/a)]/E(1/a^2) \tag{1}$$

where $E[\cdot/]$ and $E(\cdot)$ are the incomplete and complete elliptical integrals of the second kind, respectively. After additional manipulation it can be shown that

$$D = (K(1-1/a^2) - E(1 - 1/a^2)/E(1/a^2) \tag{2}$$

where $K(\cdot)$ is the complete elliptical integral of the first kind using complex variable theory and applying the boundary conditions as

$$Z \to \infty \ , \ U \to U_0 \text{ and } V \to 0 \tag{3}$$

results in the irrotational velocity components in the Z -plane equal to

$$U - iV = Af'(z) \tag{4}$$

where

$$f'(z) = AE(1/a^2)\,[(\lambda^2 - 1)/(\lambda^2 - a^2)]^{\frac{1}{2}} \tag{5}$$

and

$$A = U_0/a\ E(1/a^2) \tag{6}$$

In the real flow, the action of viscosity is to induce an additional force which causes the flow to separate rather than turn the corner as in the potential case. The shear layer which separates the outer potential flow from the more quiescent fluid within the cavity is highly rotational and unstable with a tendency to roll up into concentrated regions of high vorticity due to the Kelvin Helmholtz instability.

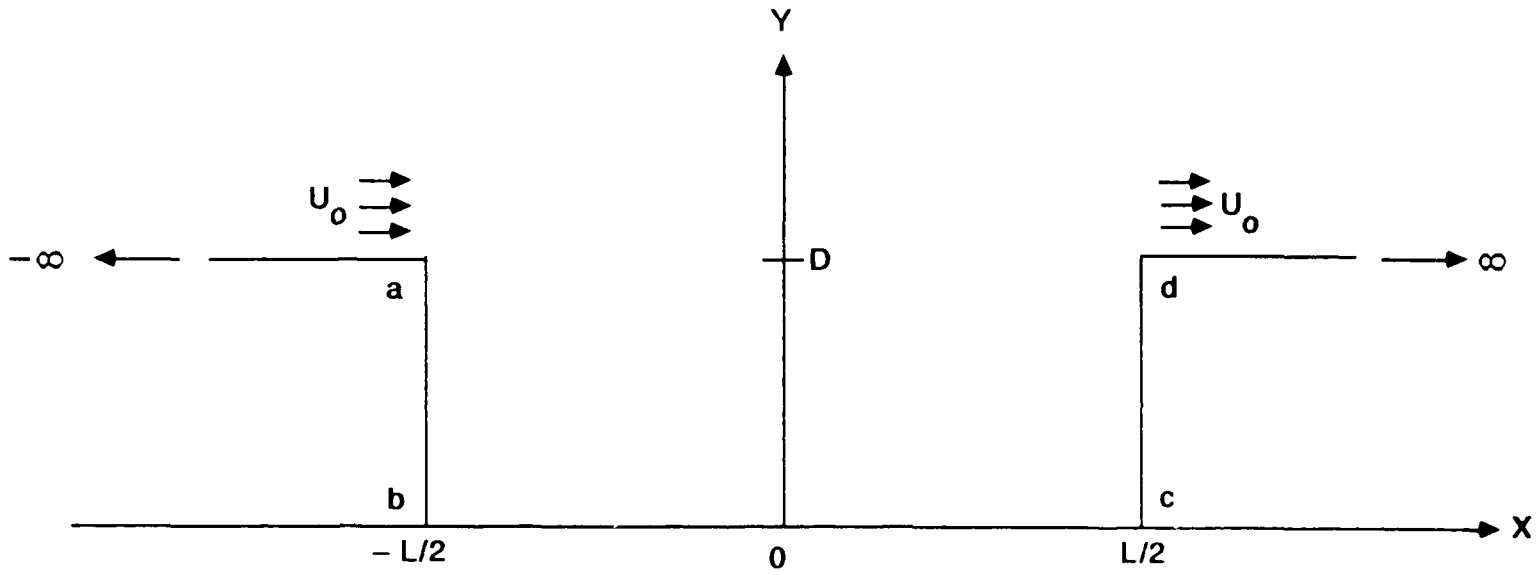

Figure 1. A Two-Dimensional Cavity Geometry

Suppose that, at time t, there exists N vortices of strength Γ_j; located at positions (Z_j (j = 1,2,...N). The velocity field will be the superposition of that induced by the totality of vortices on to the cavity flow which results in:

$$U - iV\Big|_{\bar{z} = \bar{z}_k} = \left[A - \frac{i}{2\pi}\sum_{\substack{j=1\\ j\neq k}}^{N}\left(\frac{\Gamma_j}{\lambda_k - \lambda_j}\right) + \frac{i}{2\pi}\sum_{\substack{j=1\\ j\neq k}}^{N}\frac{\Gamma_j}{\lambda_k - \lambda_j^*}\right]$$

$$+\left[\frac{i}{2\pi}\sum_{\substack{j=1\\ j\neq k}}^{N}\frac{\Gamma_j}{(\lambda_k - \lambda_j^*)}\right] f'(\bar{z}_k)\Big] - i\frac{\Gamma_k}{4} f''(\bar{z}_k)\Big/ f'(\bar{z}_k) \qquad (7)$$

where the image vortices are included to satisfy the boundary condition of zero velocity through the cavity walls, and Z_k is the point of interest.

MODIFICATION BY ARTIFICIAL VISCOSITY

Significant irregularities which can occur in the velocity field arise when the concentration of vortices increases in a particular flow region. These irregularities seem to be caused when one point vortex's trajectory brings it close to a second point vortex. The result is a rapid circling motion. In a viscous fluid, the velocity field induced by a single vortex is diminished in magnitude. Thus, a viscous vortex is used in place of the inviscid model, that is

$$V_\theta = \frac{\Gamma}{2\pi r}\left[1 - \exp\left(\frac{-r^2}{4\nu t}\right)\right] \qquad (8)$$

$$V_r = 0 \qquad (9)$$

where V_θ and V_r are the angular and radial velocity components. r is the distance from the vortex center, and t is chosen such that a point vortex results when t = o. Upon substitution into the cavity velocity field expression results in:

$$U - iV\Big|_{\bar{z} = \bar{z}_k} = \left[A - \frac{i}{2\pi}\sum_{j=1}^{N}\frac{\Gamma_j}{\lambda - \lambda_j}\left(1 - \exp\left(-\frac{[\lambda - \lambda_j]^2}{4\nu t}\right)\right)\right.$$

$$\left. + \frac{i}{2\pi}\sum_{\substack{j=1\\ j\neq k}}^{N}\frac{\Gamma_j}{(\lambda - \lambda_j^k)}\left(1 - \exp\left(-\frac{[\lambda - \lambda_j^*]^2}{4\nu t}\right)\right)\right] f'(\bar{z}_k) - i\frac{\Gamma_k}{4} f''(\bar{z}_k)\Big/ f'(z_k) \qquad (10)$$

This equation is not exact since it is not compatible with the Navier Stokes equation due to its nonlinearity. For a sufficiently large N and a suitable chosen value of the artificial viscosity, a more regular pattern of vortex motion results along with a smoother and more realistic velocity field.

MODIFICATION OF VORTICITY NEAR SEPARATION

Prandtl (Reference 29) has shown that the separation from an infinite cylinder can be delayed or prevented by rotation of the cylinder such that the tangential velocity is in the same direction as the outer flow. Catalano and Viets (Reference 30) have found that a quasi-cylinder with counter flow rotation can also have a significant beneficial effect in delaying separation. In both cases the vorticity near the separation point is modified, diminished by parallel rotation, amplified by counter rotation. In the introduction, reference is made to the reduction of oscillations in cavities by insertion of fences upstream of the cavity leading edge which modify the velocity profile near separation. Thus, there is a direct analogy between the effects of fences and the effect of a rotating cylinder. To include the ability of the discrete vortex model to incorporate the rotating cylinder effects, a Hankel transform is used to solve the unsteady vorticity equation with the solution given as the following Fourier-Bessel integral:

$$V_\theta = \frac{4\omega\sqrt{\nu}}{\pi}\int_0^\infty \frac{\left[J_0(\lambda R)\, Y_1(\lambda r/\sqrt{\nu}) - Y_0(\lambda R)\, J_1(\lambda r/\sqrt{\nu})\right]\left[1 - \exp(-\lambda^2 t)\right]}{J_0^2(\lambda R) + Y_0^2(\lambda R)} \frac{d\lambda}{\lambda^2} \quad (11)$$

A detailed derivation is presented by Catalano and Shih (Reference 31).

BOUNDARY CONDITIONS

The image vortices in Equation (10) are used to satisfy the zero velocity condition at the walls. Clements (Reference 24) and Hardin and Mason (Reference 25) suggested vortices which are closer than 0.015 to the cavity walls. This procedure has been adopted in this investigation. Clements (Reference 24) commented that the removal of the vortices is equivalent to the viscous dissipation of the vorticity, that is the no-slip condition creates high frequency vortices near the boundary, which accelerates the dissipation of energy close to the walls. The potential flow solution is then modified to account for viscous effects.

NUMERICAL ERROR

The discrete vortex model approximates a sheet by a series of individual points. The model is extremely sensitive to the time interval, between the successive vortices shed at the leading edge. Hardin and Mason (Reference 25) selected the dimensional time step, $U_0\Delta t$, such that $0.01 \leq U_0 \Delta t \leq 0.3$. This criterion has been incorporated into the present work (Figure 2).

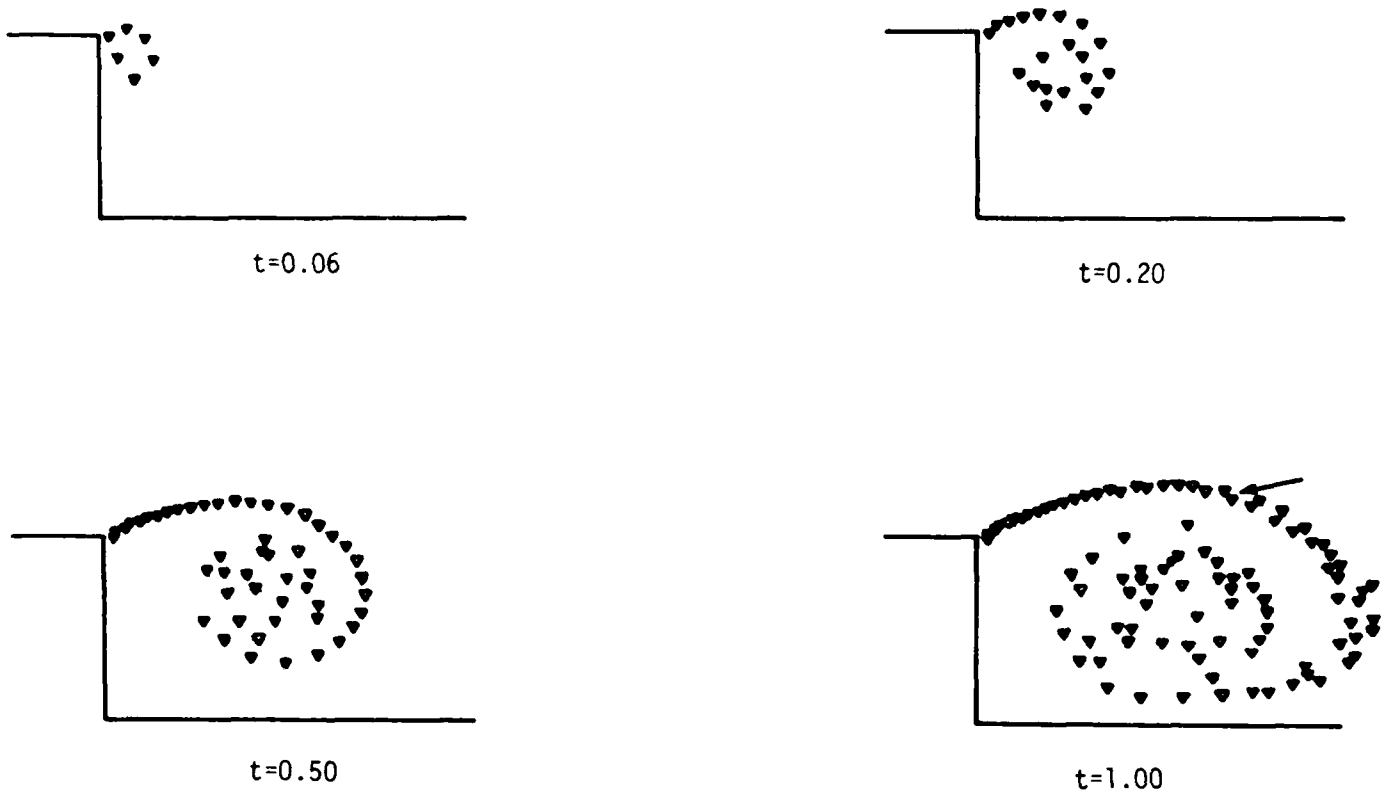

Figure 2. The Motion of a Rolling-Up Vortex at $\Delta t=0.01$ and U_o = 3m/s (A/R=0.25)

SECTION III
EXPERIMENTIAL DESIGN AND PROCEDURE

A cavity model (Figure 3) with fixed depth, D, equal to 5 cm, fixed width, W, equal to 5 cm and variable length, L, is mounted in a splitter plate 30 cm wide by 56 cm long. The plate is carefully contoured to limit the disturbances that result when the model is mounted in the test section of a subsonic tunnel having dimensions 46 cm by 92 cm by 184 cm in length. The blockage is calculated to be approximately 5 percent. The length which can be varied from 5 cm to 35 cm is accomplished via sliding blocks. The tunnel free stream turbulence intensity is approximately 0.5 percent at a wind speed of 6m/sec. The incoming flow condition is determined for the location close to the leading edge of the cavity. Note that the cavity leading edge is 20 cm downstream from the splitter plate leading edge, with the resulting Reynolds numbers equal to $Re_x = 8 \times 10^4$, $Re_{crit} = 10^6$, $Re_\delta = 5.5 \times 10^3$ and with a laminar upstream boundary layer. The boundary layer thickness is calculated to be approximately 1 cm. Wool tufts and oil film flow visualization are utilized to observe the complicated three dimensional patterns within the cavity. The cavity bottom is replaced with optical-quality glass to permit line-of-sight for photography. A motor transmission oil with naptha and colored dyes is used as the streaking medium.

Hot wire anemometry and a laser Doppler velocimeter (LDV) are used to measure mean velocity and turbulent intensity profiles in the longitudinal and normal directions. The LDV is a DISA single component, back scatter set-up using a frequency tracker and a 7.5 mwatt helium-neon coaxial laser. Olive oil in conjunction with an agricultural fogger is used to provide light scatters with a diameter of 0.5 microns.

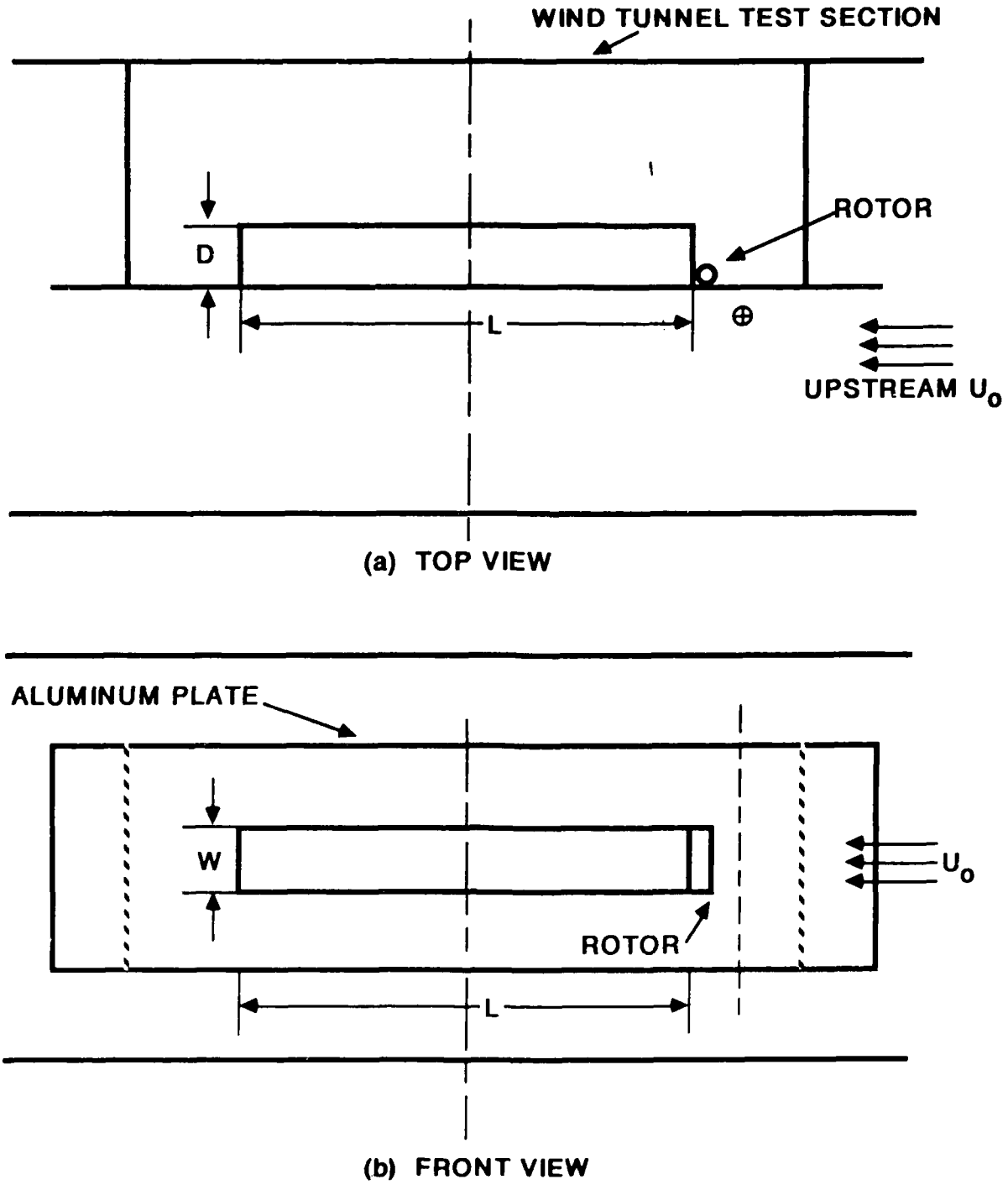

Figure 3. A Schematic Description of the Cavity Model Installed at the Test Section of the Wind Tunnel

SECTION IV
RESULTS AND DISCUSSION

1. FLOW PATTERN

The evidence of three dimensional flow and one effect of a finite width is shown in Figure 4. The oil flow patterns on the cavity flow correspond to L/D = 2, 3, and 4. Note that as the L/D ratio increases, the parabolic velocity profile becomes more pronounced. This is in accord with Maull and East who observed that a wave flow pattern first appears when W/L = 9.0. For the present case W/L = 1. The oil film results and woolen tuft behavior suggest the fluid behavior in Figure 5 (a)-(b). Experimental data confirm these results though the analytical model (Figure 6) fails to indicate the existence of secondary rotational flow in the cavity corners.

2. MEAN VELOCITIES

Here, the nondimensionalized longitudinal, mean velocity, U/U_{max} is plotted versus the nondimensionalized transverse location Y/D, where U_{max} is the free stream speed.

A comparison between the analytical model predictions and the experimentally determined results is shown in Figure 7, for different downstream locations. For these comparisons, the artificial viscosity is set equal to zero. Note that while the agreement is reasonable with respect to location of the core of the expected vortex ($U/U_{max} = 0$), there exists a consistent trend to exaggerate the amplitude of the mean velocity within the cavity in both the downstream and upstream locations. This would suggest that an introduction of a nonzero ν_a in the vortex model would help alleviate the discrepancy. In fact, Figure 8 demonstrates the effect of ν_a on the mean velocity profiles at 2 X/L = 0, and establishes a possible source of error in Figure 7 to be the inviscid assumption. The agreement between analytical predictions and experimental data improves for all $\nu_a > 0$.

The nondimensionalized, transverse, mean velocity, V/U_{max}, is plotted versus y/D for several downstream locations in Figure 9. Once again the analytical predictions exaggerate the strength of the vortex core. An increase in the artificial viscosity does aid to a certain extent as in the longitudinal case. The model does predict the correct behavior: a positive mean transverse velocity then changes sign as the flow proceeds downstream.

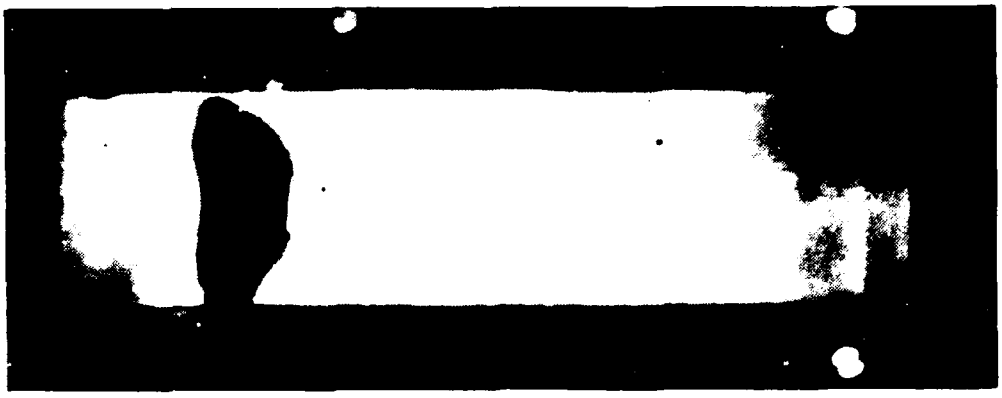

(a) $D/L = 0.25$

(b) $D/L = 0.33$

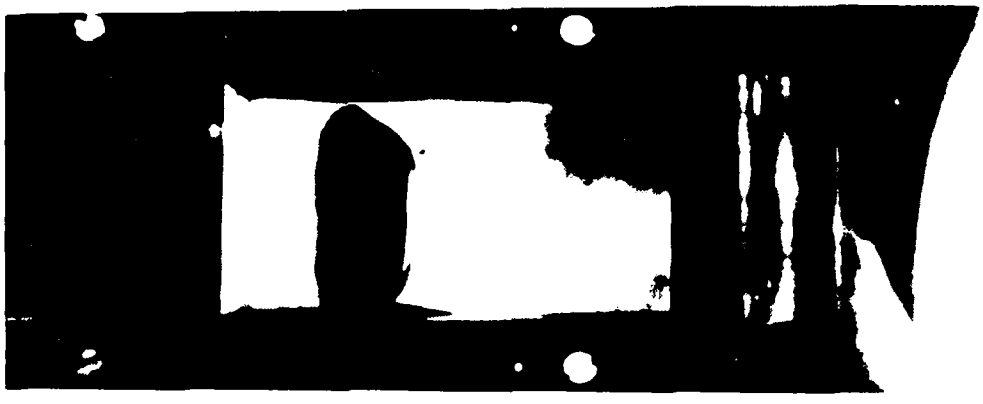

(c) $D/L = 0.50$

Figure 4 : Oil flow patterns on the cavity bottom

: free-stream direction from right to left

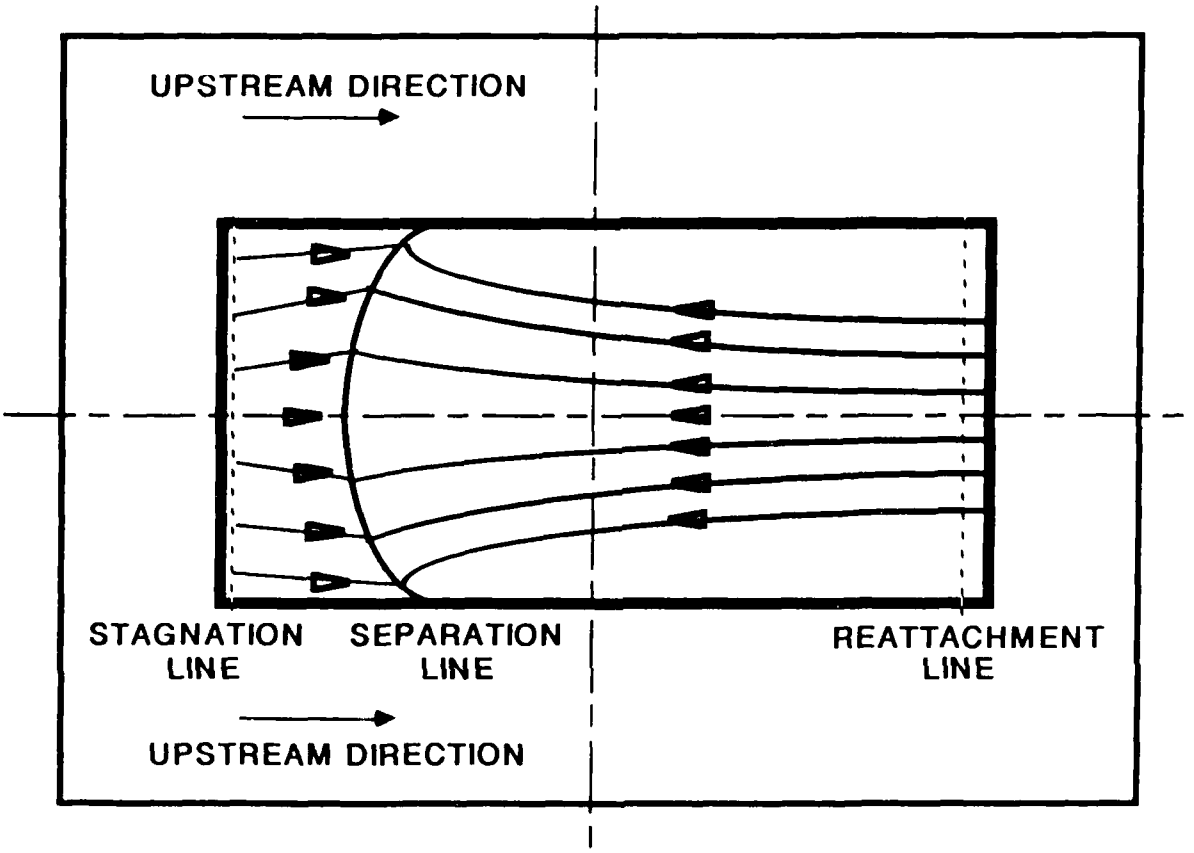

Figure 5a. Streamlines at the Cavity Bottom

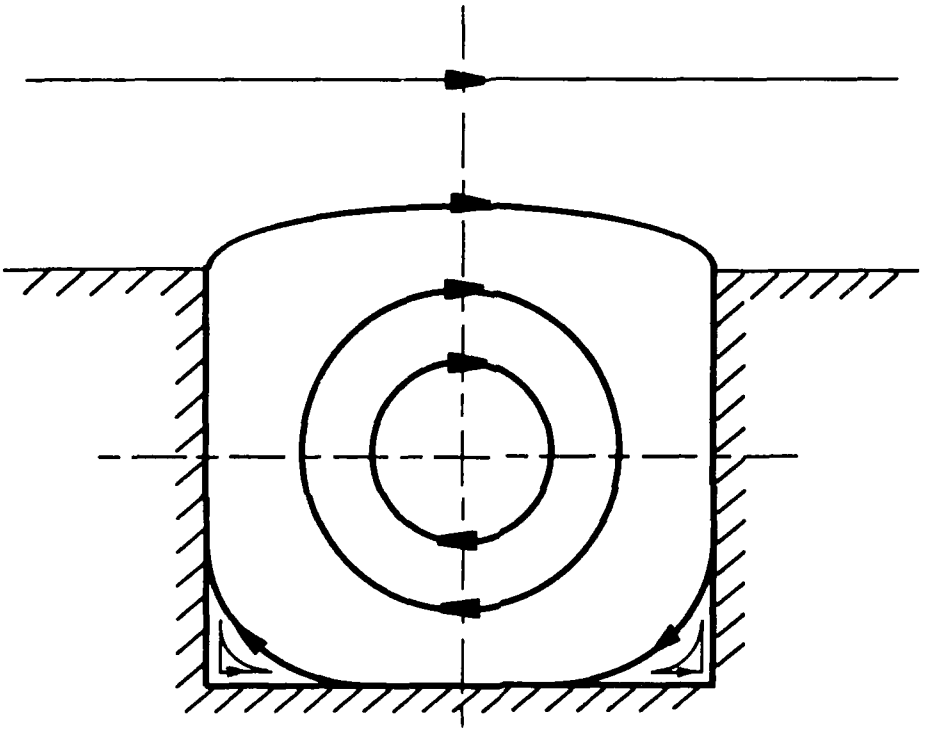

Figure 5b. Streamlines at the Cavity's Center Surface

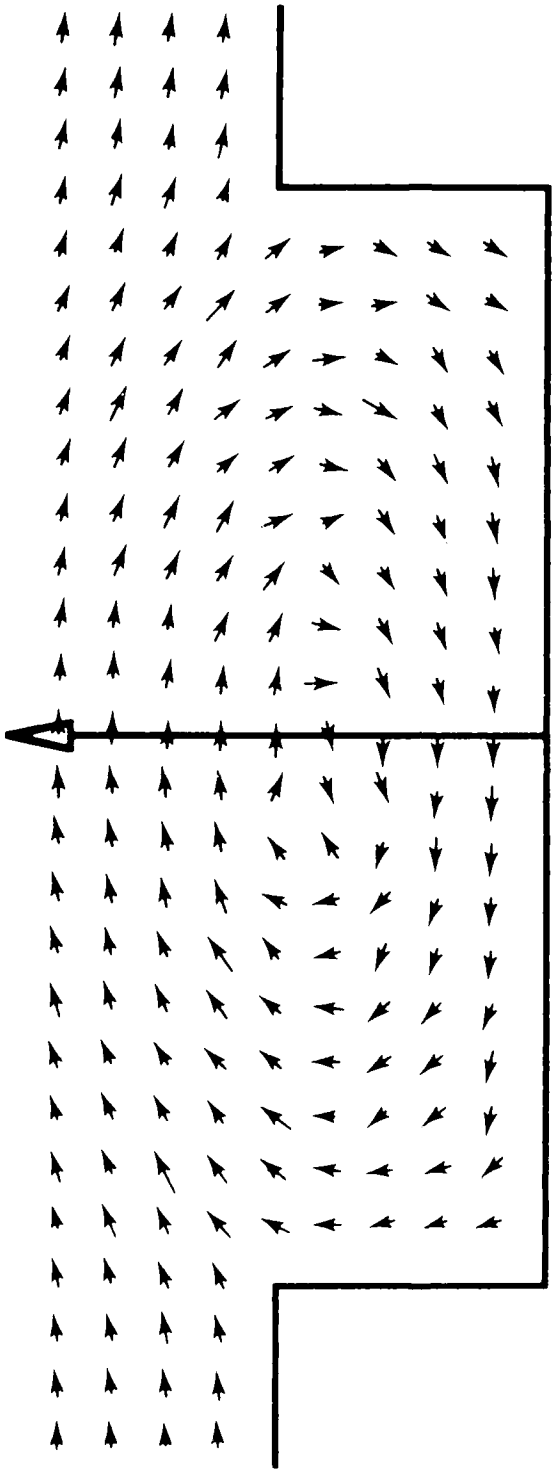

Figure 6. Instantaneous Distribution of Velocity Vectors at the Final Stage (t=3.0)

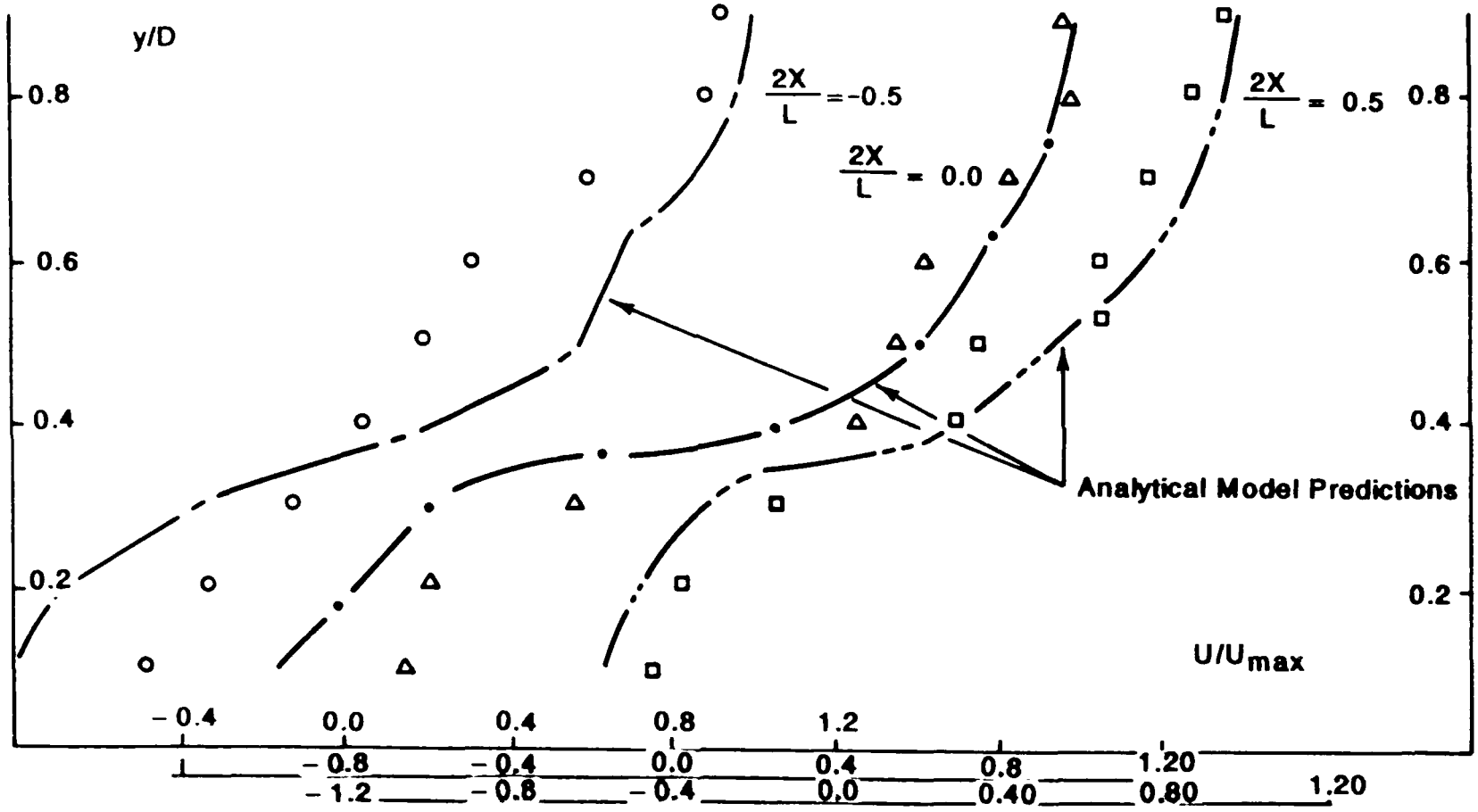

Figure 7. Comparison Between Experimental and Analytical Results

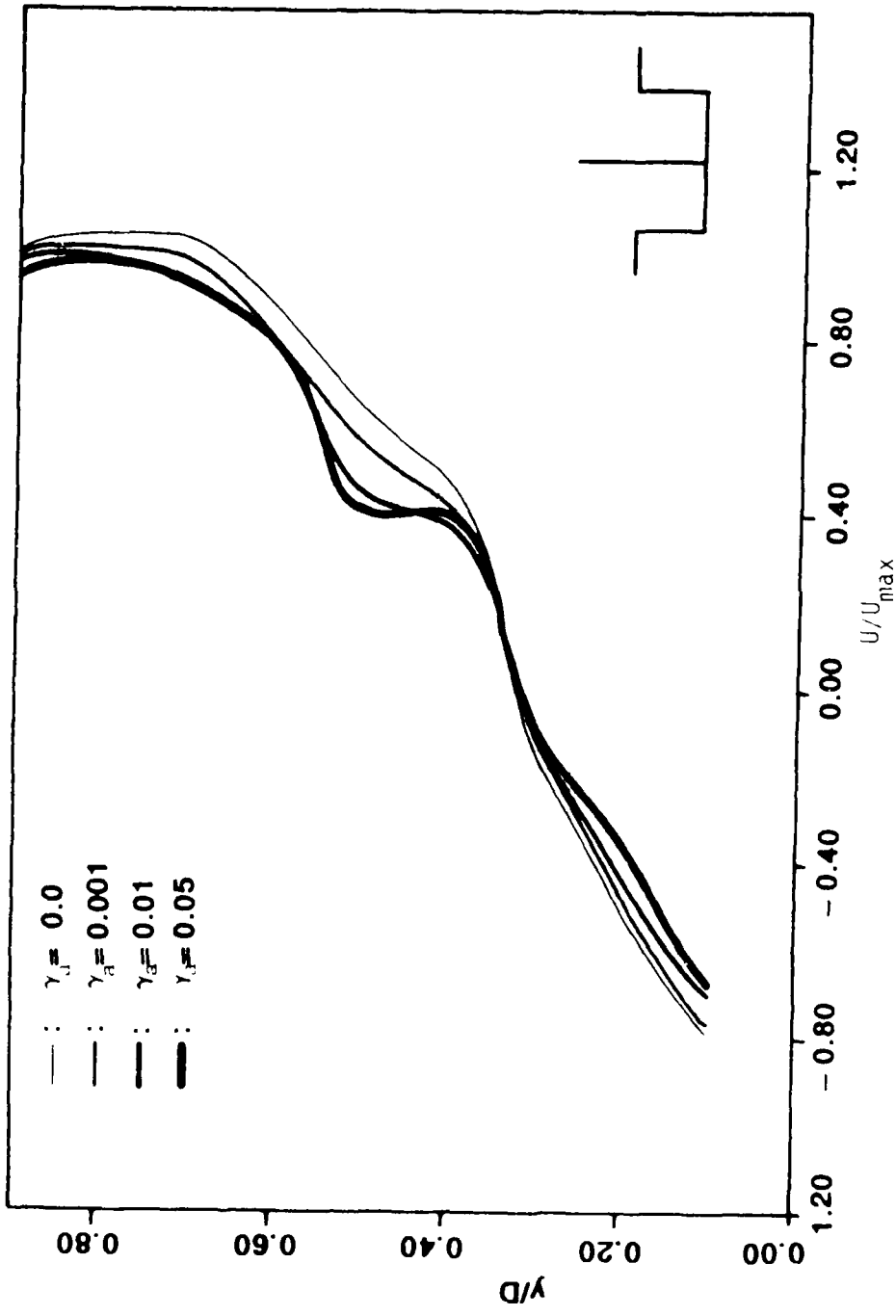

Figure 8. Effect of Artificial Viscosity γ_a

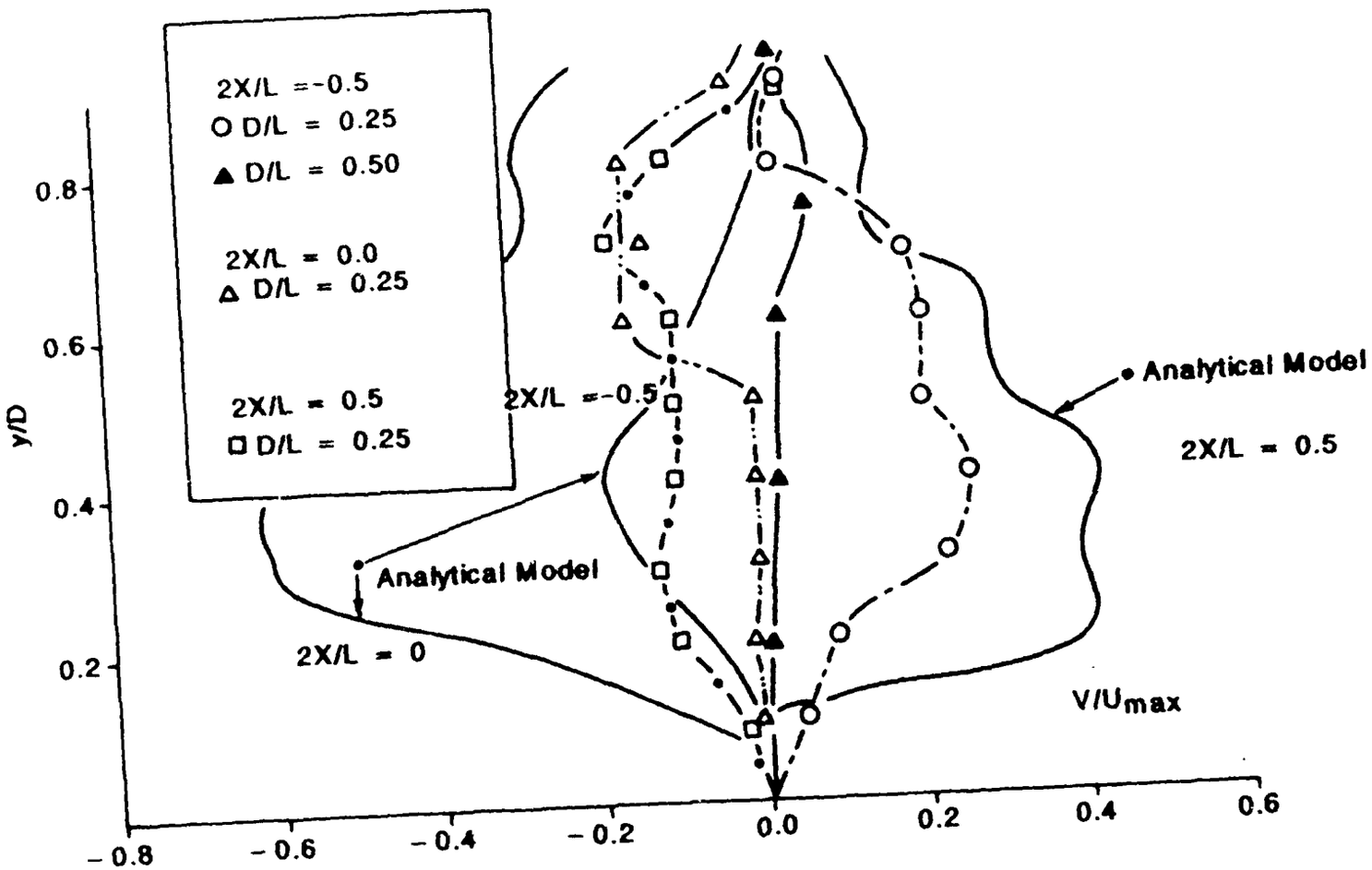

Figure 9. Transverse Velocity Comparison Between Experiment and Analytical Model

Recall that the experimental data is at the centerline of a 3-D flow field while the model is based on a 2-D assumption. One of the stated goals of the investigation was to examine the effects of finite span. A comparison of the present work to previous 2-D cavity results is shown in Figure 10. Several observations can be made. First, note that the center of the vortex trapped within the cavity is lower (i.e., $Y_{3\text{-D Core}} < Y_{2\text{-D Core}}$) for the 3-D case. Hence, the ratio of width to length, W/L, is equally as important as D/L in characterizing the flow. Also, for the 3-D case, as W/L decreases from 0.5 to 0.25 the vortex center is pushed still farther into the cavity. Additionally, the mean velocity gradient increases in magnitude within the cavity as does the strength of the separation region.

3. TURBULENT INTENSITIES

Longitudinal turbulent intensities, $(u^2)^{\frac{1}{2}}/U_{max}$ are plotted versus transverse location, y/D, for three different downstream locations in Figure 11. Note the downstream development with the turbulence first slightly increasing from 2 X/L = -0.5 to 2 X/L = 0, and then significantly decreasing at 2 X/L = 0.5. This trend is also shown in the downstream development of the transverse turbulent intensities $(v^2)^{\frac{1}{2}}/U_{max}$, which are shown in Figure 12. The data suggests a gradual increase in turbulence as the flow proceeds from the leading edge of the cavity towards the centerline with a more rapid decrease as the rear wall becomes nearer in proximity.

The experimental data from the present 3-D case are also compared to the analytical model predictions and to previous 2-D investigations in Figure 13, for both the longitudinal and transverse cases. Note the reasonable agreement exists between the 3-D data and the predictions. However, both results are considerably higher than the infinite span case. The reason for the differences may be found in the use of laser velocimetry versus hot wire anemometry or be the consequence of the finite span.

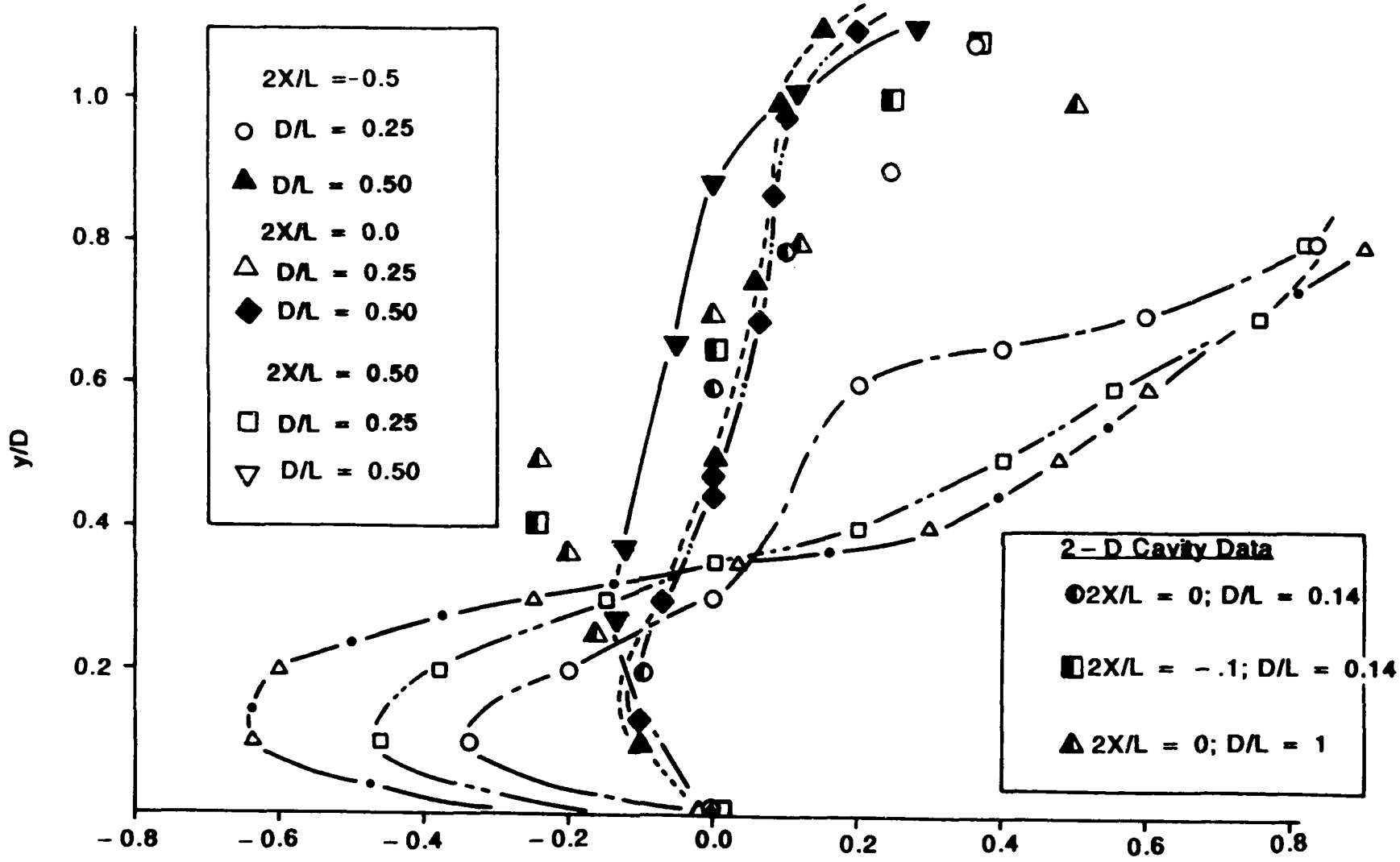

Figure 10. Comparison with Previous Investigations of Mean Velocity Profiles

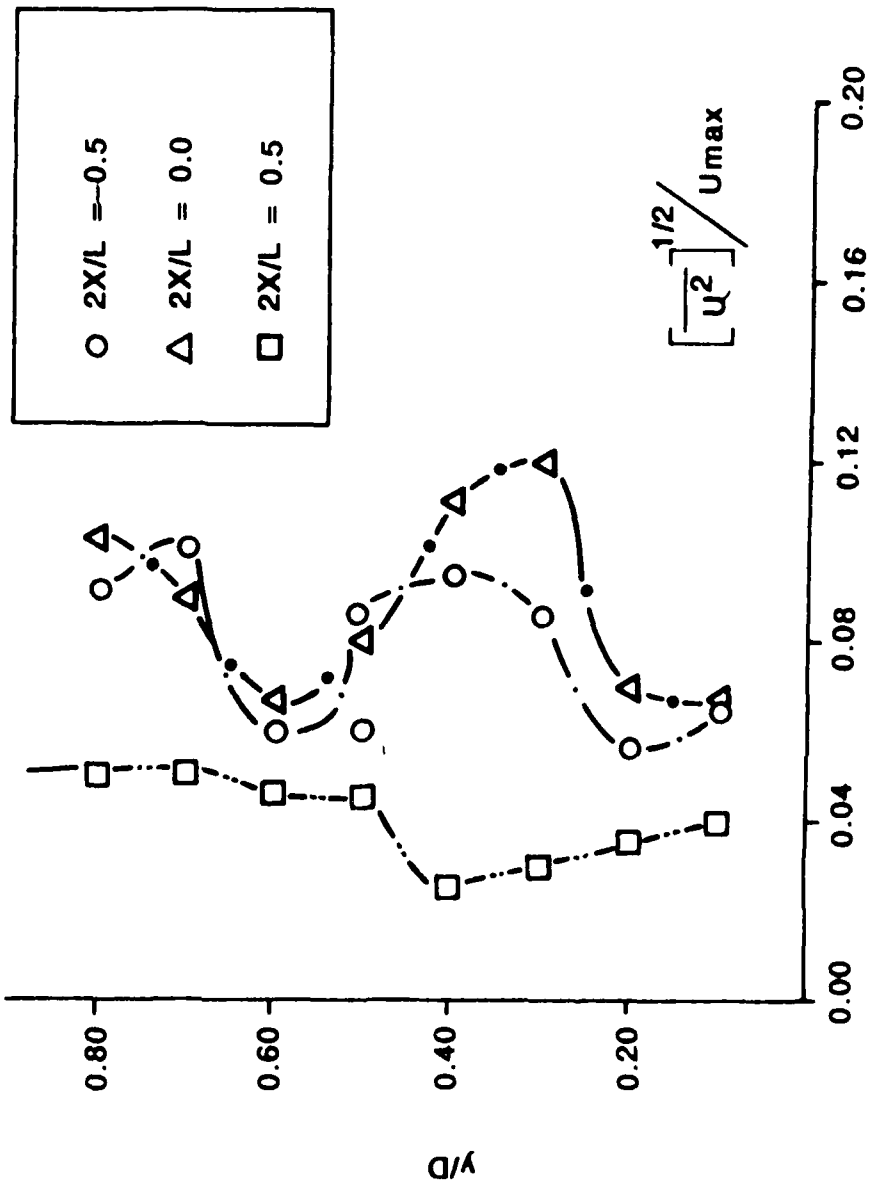

Figure 11. Turbulent Intensities in 3-D Cavity

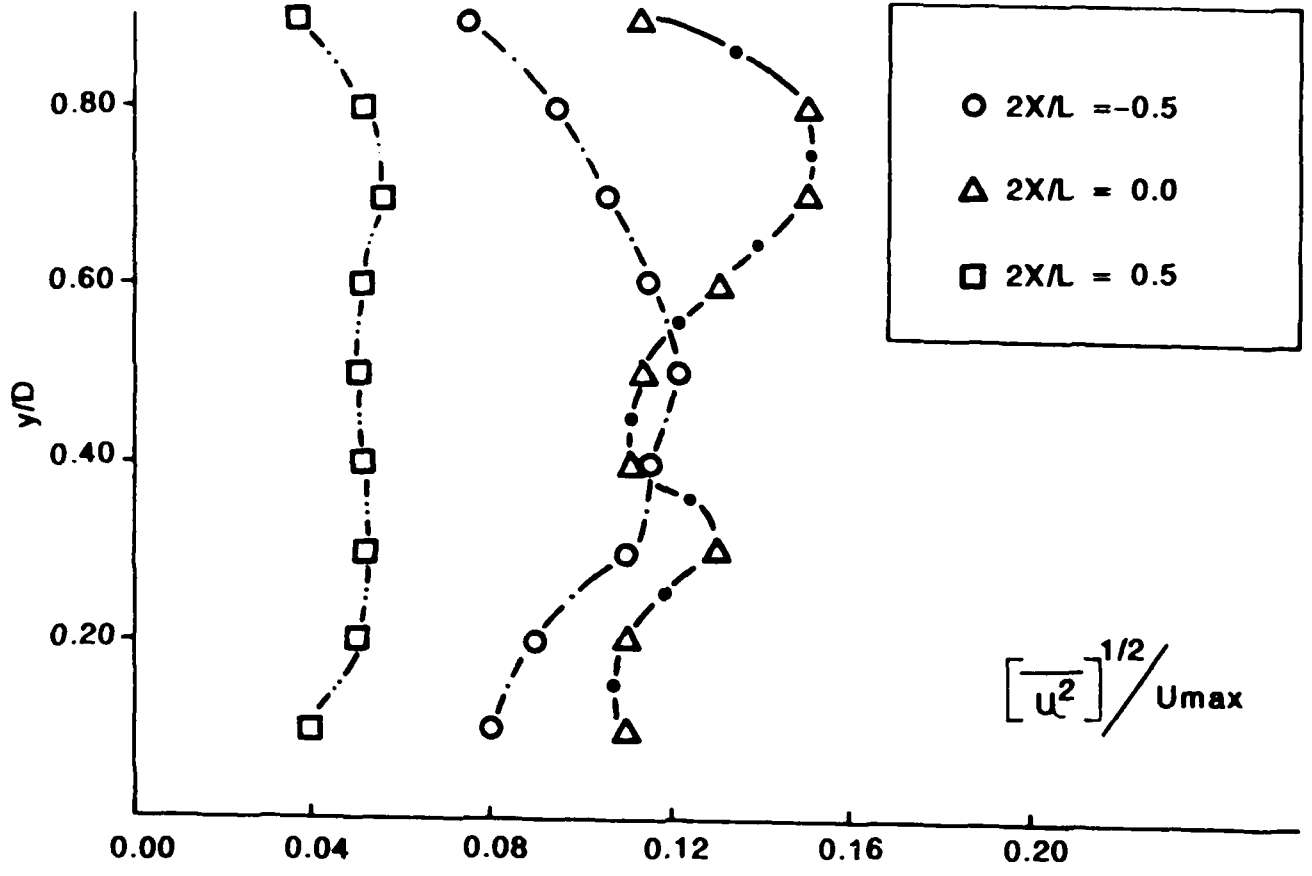

Figure 12. Transverse Turbulent Intensities in 3-D Cavity

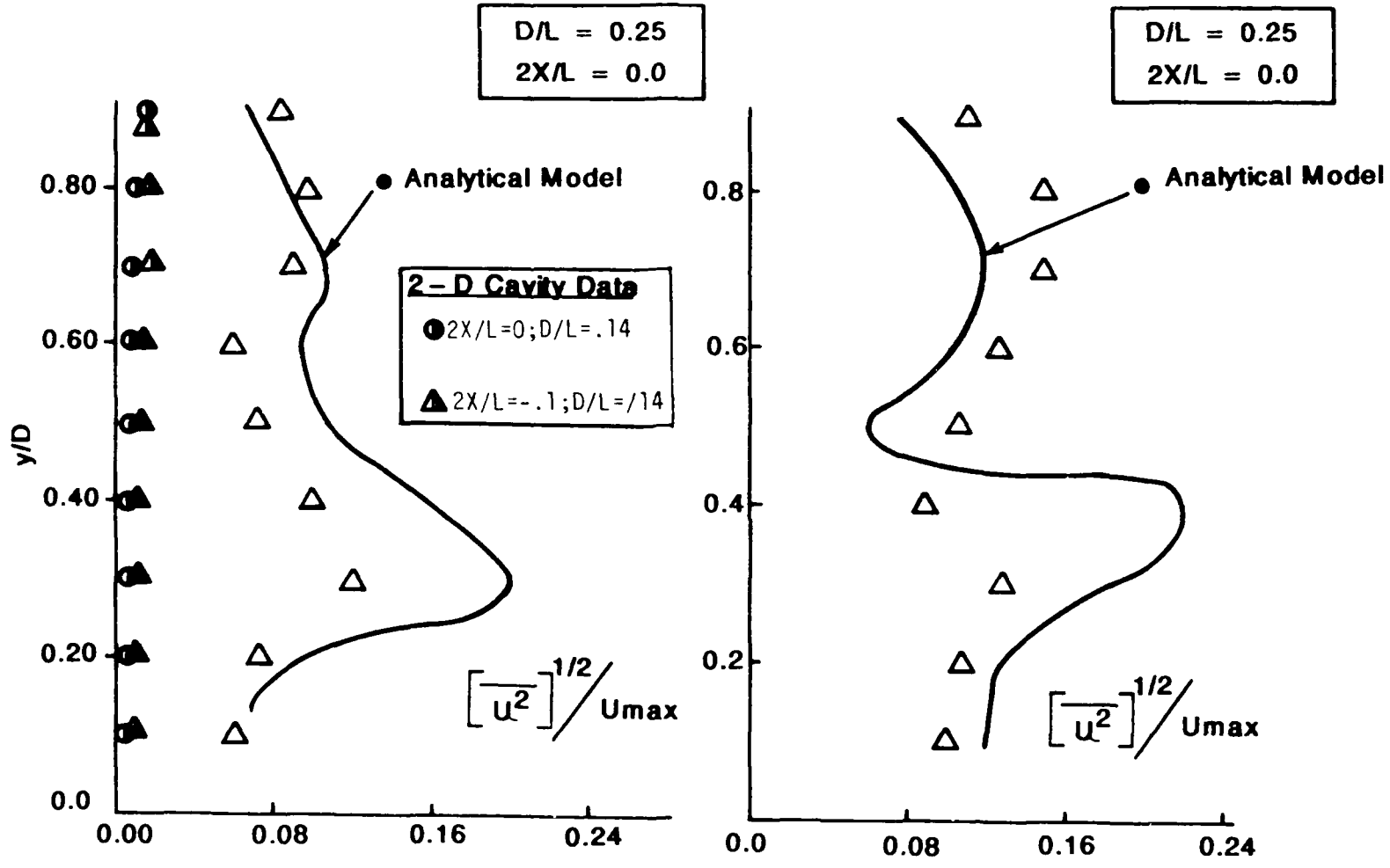

Figure 13. Comparison of Experimental and Analytical Model Results

SECTION V
CONCLUSIONS

A comparison between 2-D and 3-D Cavity experimental data has been documented in the present investigation. In addition, an analytical model has been developed and evaluated for application to 3-D cavity flows. The following conclusions have been reached:

1. Flow visualization techniques indicate that as the ratio, L/D increases for a fixed W/L, the parabolic shape of the mean velocity profile becomes more pronouned.

2. The analytical model fails to predict secondary rotational flows in the cavity corners in contradistinction to experimental evidence.

3. The analytical model predictions for the longitudinal and lateral mean velocities are improved with the introduction of an artificial viscosity, ν_a, into the vortex model. This suggests the increased importance of viscosity as the cavity width is decreased.

4. The central vortex core location is found to move deeper within the cavity for a finite and fixed width as the length is increased.

5. The turbulent intensities in both the longitudinal and transvers direction are several times higher at the centerline of the 3-D cavity than for the 2-D case. The analytical model predictions and experimental data corroborate this observation.

SECTION VI
RECOMMENDATIONS

1. The analytical model based on the superposition of potential flow and a viscous point vortex model has shown considerable promise in the prediction of the centerline flow in a 3-D embedded cavity. The artificial viscosity concept was demonstrated as a key device in improving the agreement even further. Much work needs to be done in optimizing the value of the artificial viscosity and in understanding its dependency on flow parameters.

2. The analytical model fails to predict the secondary and tertiary vortex-like corner flows. This short coming is perhaps due to the adhoc assumptions concerning the boundary layer. Work should be done to attempt to model the boundary layer perhaps by an integral technique and then match the boundary layer to the outer cavity flow. This might provide insight into the viscosity dominated corner regions of the flow field.

3. The predictions of mean velocities and turbulent intensities are merely the first and second steps of the work to be accomplished. Several other parameters should be calculated such as auto correlations of the fluctuating velocity field which would provide insight into the development of the integral length scales and the Taylor microscales. Of paramount interest would be the auto spectral density functions which can be obtained via Fourier transforming the auto correlations. The auto spectra would indicate the extent of structure in the turbulent flow. This turbulent structure is important as it relates to the existence of self-sustaining oscillations in the cavity.

4. Much work is needed to better understand the difference between two-dimensional and three-dimensional cavity flows. The initial evidence presented here suggests a radical difference between the two flows. The sensitivity of the cavity to length/depth and length/width ratios must be carefully documented.

(The reverse of this page is blank)

REFERENCES

1. Kawagutti, M., "Numerical Solution of the Navier-Stokes Equation for Flow into a Two Dimensional Cavity," Journal of the Physical Society of Japan, Vol. II, December 1961, pg. 2307-2315.

2. Mills, R. D., "Numerical Solution of the Viscous Flow Equations for a Class of Closed Flaws," Journal of the Royal Aeronautical Society, Vol. 69, October 1965, pp. 714-718.

3. Burgraf, O. R., "Analytical and Numerical Study of the Structure of Steady, Separated Flows," Journal of Fluid Mechanics, Vol. 24, January 1966, pp. 113-151.

4. Pan, F. and Acrivos, A., "Steady Flow in Rectangular Cavities," Journal of Fluid Mechanics, Vol. 28, June 1967, pp. 643-655.

5. Nallaswamy, M. and Prasad, K. K., "On Cavity Flow at High Reynolds Number," Journal of Fluid Mechanics, Vol. 79, February 1977, pp. 391-414.

6. Bozeman, J. D. and Dalton, C., "Numerical Study of Viscous Flow in a Cavity," Journal of Computational Physics, Vol. 12, July 1973, pp. 348-363.

7. Sarohia, V., "Experimental Investigation of Oscillation in Flow Over Shallow Cavities," AIAA Journal, Vol. 15, July 1977, pp. 984-991.

8. Roshko, A., "Same Measurements of Flow in a Rectangular Cutout," NASA TM-3488, August 1955.

9. Tani, S., Suchi, M. and Komodo, M., "Experimental Investigation of Flow Separation Associated with a Step or Groove," Aeronautical Research Institute, University of Tokoyo, No. 364, April 1961.

10. Sinha, S. N., Gupta, A. K., and Oberai, M. M., "Laminar Separating Flow Over Backsteps and Cavities, Part 2, Cavities," AIAA Journal, Vol. 20, 1982, pp. 370-375.

11. Rockwell, D., and Knisley, C., "The Organized Nature of Flow Impingement Upon a Corner," Journal of Fluid Mechanics, Vol. 93, Pt., 3, August 1979, pp. 413-432.

12. Hankey, W. L. and Shang, J. S., "The Numerical Solution to Pressure Oscillations in an Open Cavity," AIAA Paper 79-0136, AIAA 17th Aerospace Sciences Meeting, New Orleans, January 5-17, 1979.

13. Gatski, T. B., Grosch, C. E., and Rose, M. E., "An Numerical Study of the Two Dimensional Navier-Stokes Equation in Vorticity-Velocity Variables," Journal of Computational Physics, Vol. 48, No. 1., October 1982, pp. 1-22.

14. Rockwell, D., and Naudascher, E., "Review-Self Sustaining Oscillations of Flow Past Cavities," J. Fluid Mechanics, Transactions of the ASME, 100, pp. 152-165, 1978.

15. Rosenhead, L., "Formation of Vortices from a Surface of Discontinuity," Proc. Roy. Soc., A134, pp. 170-192, 1931.

16. Birkhoff, G. D. and Fisher, J., "Do Vortex Sheets Roll Up?" Rc. Circ. Mat. Palermo Ser. 2, 8, pp. 77-99, 1959.

17. Abernathy, F. H. and Kronauer, R. E., "The Formation of Vortex Sheets," J. Fluid Mechanics, 13, pp. 1-20, 1962.

18. Moor, D. W., "A Numerical Study of the Roll-Up of a Finite Vortex Sheet," J. Fluid Mechanics, 63, pp. 225-235, 1974.

19. Gerrard, J. H., "Numerical Computation of the Magnitude and Frequency of the Lift on a Circular Cylinder," Phil. Trans. Roy. Soc., 261, No. 1118, pp. 137-162, 1967.

20. Sarpkaya, T., "An Analytical Study of Separated Flow about Circular Cylinder," ASME, J. Basic Engineering, 90, pp. 511, 1968.

21. Laird, A. D. K., "Eddy Formation Behind Circular Cylinders," Proc. ASCE, Hydraulic Division, 97, pp. 763, 1971.

22. Clements, R. R., "An Inviscid Model of Two-Dimensional Vortex Shedding," J. Fluid Mechanics 28, pp. 643-655, 1973.

23. Clements, R. R. and Maull, D. J., "The Rolling Up of a Trailing Vortex Sheet," Aero. J., 77, pp. 46-51, 1973.

24. Clements, R. R. and Maull, D. J., "The Representation of Sheets of Vorticity by Discrete Vortices," Prog. Aerospace Science, 16, pp. 129-146, 1975.

25. Hardin, J. C. and Mason, J. P., "Broadband Noise Generation by a Vortex Model of Cavity Flow," AIAA Journal, 15, pp. 632-637, 1976.

26. Davies, P. O. A. L., Hardin, J. P., Edwards, A. V. J., and Mason, J. C., "A Potential Flow Model for Calculation of Jet Noise," AIAA Paper 75-441, Hampton, VA, March 1975.

27. Bradshaw, P. Ferris, D. H. and Johnson, R. F., "Turbulence in the Noise-Producing Region of a Circular Jet," J. Fluid Mechanics, 19 pp. 591-624, 1964.

28. Kuwahara, K. and Tokami, H., "Numerical Studies of Two Dimensional Vortex Motion by a System of Point Vortices," J. Phys. Soc., Japan 34, pp. 247-253.

29. Goldstein, T., Modern Developments in Fluid Dynamics, Vol. 1, Dover, NY, pp. 79, 1965.

30. Catalano, G. D. and Viets, H., "Drag Reduction by Unsteady Vortex Shedding Behind a Bluff Body," 19th AIAA Aerospace Sciences Meeting, January 1984.

31. Catalano, G. D. and Shih, C., "A Time Dependent Vortex Shedding Model," Il Nuovo Cimento, June 1984.

(The reverse of this page is blank)

END

4-87

DTIC